Chalcogenide Letters

Tech Science Press

http://doi.org/10.32604/cl.2026.075947

ARTICLE

Growth Techniques and Phase Characterization of $Sn_{1-x}Er_xTe$ Crystals

Mammadov Israil Musa*

Faculty of Physics, Azerbaijan State Pedagogical University, 68 U. Gadzhibekli Str., Baku, Azerbaijan
*Corresponding Author: Mammadov Israil Musa. Email: israil.memmedov.66@bk.ru

Received: 11 November 2025; Accepted: 26 February 2026; Published: 09 May 2026

ABSTRACT: Erbium-doped SnTe ($Sn_{1-x}Er_xTe$) single crystals were synthesized to investigate the influence of erbium incorporation on phase stability, crystal structure, and thermophysical behavior relevant to thermoelectric applications. Single crystals with nominal compositions x = 0.00–0.10 were grown using the vertical Bridgman technique under controlled thermal conditions. X-ray diffraction analysis confirmed that at low erbium concentrations ($x \leq 0.02$–0.03), erbium is substitutionally incorporated into the cubic NaCl-type SnTe lattice without detectable secondary phases. At higher erbium contents ($x \geq 0.05$), Er-rich secondary phases such as ErTe and Er_2Te_3 precipitate within the SnTe matrix, indicating a limited solubility of erbium in SnTe. Differential thermal analysis revealed reproducible thermal effects associated with phase transformations and the formation of secondary phases at elevated dopant concentrations. Scanning electron microscopy combined with energy-dispersive spectroscopy showed microstructural refinement and increased defect density with increasing erbium content. Moderate erbium incorporation enhances phonon scattering, resulting in reduced lattice thermal conductivity and an increased Seebeck coefficient, whereas excessive doping leads to phase instability and degradation of electrical transport. These results demonstrate that erbium acts as an effective dopant for tuning the thermoelectric properties of SnTe within a narrow compositional window, while exceeding the solubility limit induces multiphase behavior and structural instability. The study provides experimentally grounded guidelines for controlled rare-earth doping and phase stability optimization in SnTe-based thermoelectric materials.

KEYWORDS: Erbium doping; SnTe single crystals; phase stability; differential thermal analysis; microstructural evolution; thermoelectric properties

1 Introduction

Tin telluride (SnTe) is a narrow-gap IV–VI semiconductor that has attracted considerable attention due to its promising electrical and thermoelectric properties, relatively simple crystal structure, and lead-free composition. These characteristics make SnTe a potential alternative to conventional PbTe-based materials in thermoelectric devices, infrared detectors, and topological insulator applications [1,2]. Moreover, the physical properties of SnTe can be effectively tuned through stoichiometric control, alloying, and doping, which significantly broadens its technological relevance.

Despite its advantages, pristine SnTe exhibits a relatively low thermoelectric figure of merit (ZT), mainly due to high hole concentration and lattice thermal conductivity. Consequently, extensive research efforts have focused on enhancing its thermoelectric performance through band structure engineering, nanostructuring, and chemical doping [3–5]. Among these approaches, doping with rare-earth (lanthanide) elements has emerged as an effective strategy to modify carrier concentration, introduce resonant electronic states, and enhance phonon scattering, thereby improving thermoelectric efficiency [6,7].

Lanthanide-doped SnTe systems, including Ce-, Nd-, and Yb-doped compounds, have demonstrated improved thermoelectric properties and enhanced thermal stability at elevated temperatures [8–10]. These improvements are commonly attributed to lattice distortion arising from ionic radius mismatch, resonant level formation near the Fermi energy, and increased phonon scattering. In addition, lanthanide incorporation can significantly affect phase stability and microstructural evolution, which are critical factors for long-term device performance.

In comparison with other lanthanides, erbium (Er) doping in SnTe has been relatively underexplored. The incorporation of Er ions, which differ from Sn in both ionic radius and valence state, is expected to alter the crystal lattice, influence carrier transport, and potentially lead to secondary phase formation or structural modifications [11]. However, most existing studies on Er-doped SnTe are limited to bulk or polycrystalline samples, and systematic investigations of single-crystal growth and phase composition remain scarce.

Understanding the growth conditions and phase behavior of $Sn_{1-x}Er_xTe$ single crystals is essential for optimizing synthesis routes and tailoring material properties for thermoelectric applications. In this context, differential thermal analysis (DTA) represents a powerful tool for studying phase transformations, thermal effects, and phase equilibria. DTA enables the identification of phase transitions, reaction enthalpies, and stability regions, providing critical insight into the thermodynamic behavior of doped semiconductor systems [12,13].

Furthermore, SnTe and its structural analogues, such as GeTe and PbTe, as well as their solid solutions, continue to play a key role in the development of thermoelectric generators. Even when SnTe itself does not exhibit the highest ZT values, its compatibility with other thermoelectric materials allows it to function effectively as a component in composite and segmented thermoelectric systems [14]. Improving the performance and stability of SnTe through controlled doping therefore remains an important research challenge.

Against this background, the present study focuses on the optimized growth technology and detailed phase analysis of $Sn_{1-x}Er_xTe$ single crystals. By combining crystal growth experiments with thermal and structural characterization techniques, this work aims to clarify the role of erbium doping in modifying phase composition and stability. The obtained results are expected to contribute to a deeper understanding of dopant effects in SnTe-based materials and to provide practical guidelines for the design of efficient and thermally stable thermoelectric systems.

1.1 Crystal Growth Methods and Selection Rationale

Several synthesis techniques are available for the preparation of $Sn_{1-x}Er_xTe$ crystals, each offering specific advantages depending on the desired crystal quality, size, and compositional uniformity. Commonly used approaches include melt-based single-crystal growth methods, solid-state reactions, and vapor-phase techniques. A comparative overview of these methods is presented in Table 1.

Considering the objectives of obtaining large, compositionally uniform single crystals suitable for phase and thermal analysis, the vertical Bridgman technique was selected as the primary growth method. This approach has been demonstrated to be particularly effective for IV–VI semiconductors and their doped derivatives.

Table 1: Synthesis methods for $Sn_{1-x}Er_xTe$ crystals.

Method	Description	Advantages	Limitations	Typical Application
Bridgman method	Directional solidification from the melt in a temperature gradient	Large single crystals, good compositional control	Long growth time, strict thermal control	Single-crystal growth of SnTe and doped SnTe
Czochralski method	Crystal pulling from melt using a seed	Controlled orientation, faster growth	High equipment cost, segregation risk	High-purity SnTe crystals
Melt quenching	Rapid cooling of melt	Simple, fast	Polycrystalline material	Preliminary synthesis
Solid-state reaction	Thermal reaction of powders	Cost-effective	Limited crystal size	Precursor preparation
Vapor transport	Transport via temperature gradient	High purity	Slow, complex setup	Specialized crystal growth

1.2 Crystal Growth Conditions

Single crystals of $Sn_{1-x}Er_xTe$ (x = 0.00–0.10) were grown using the vertical Bridgman method under controlled conditions. High-purity elemental tin (Sn, 99.999%), tellurium (Te, 99.999%), and erbium (Er, 99.99%) were weighed according to the desired stoichiometric ratios and sealed in evacuated quartz ampoules ($\approx 10^{-4}$ Pa).

The ampoules were heated to approximately 1150°C, exceeding the melting temperatures of all constituents, and held at this temperature for 12–24 h to ensure complete melting and homogenization of the melt. During homogenization, periodic rocking of the ampoule was applied to promote compositional uniformity.

Crystal growth was achieved by slowly moving the ampoule through the crystallization zone at a cooling rate of 1–3°C h^{-1}, which is critical for suppressing multi-nucleation and obtaining large, defect-minimized single crystals. After crystallization, the samples were cooled to room temperature at a rate of approximately 10°C h^{-1} to reduce thermal stress and prevent cracking.

1.3 Phase and Structural Characterization Techniques

A combination of structural, microstructural, and thermal analysis techniques was employed to characterize the synthesized $Sn_{1-x}Er_xTe$ crystals.

The synthesized $Sn_{1-x}Er_xTe$ crystals were characterized using a combination of structural, microstructural, and thermal analysis techniques. These analytical methods allowed the identification of phase composition, crystal structure, morphology, and elemental distribution in the samples. The instruments used and their corresponding measurement conditions are summarized in Table 2.

XRD measurements were performed to identify crystalline phases and determine lattice parameters. SEM was used to examine surface morphology and crystal quality, while EDS provided qualitative and quantitative information on erbium incorporation and distribution. DTA measurements were carried out to identify phase transitions and thermal stability regions. For selected samples, ICP–MS and Raman spectroscopy were employed to confirm erbium concentration and probe local lattice distortions.

Table 2: Analytical methods used for characterization.

Technique	Instrument	Purpose	Measurement Conditions
X-ray diffraction (XRD)	Cu–Kα diffractometer	Phase identification, lattice parameters	$2\theta = 10^{\circ}$–80°, step 0.02°
Scanning electron microscopy (SEM)	SEM system	Morphology, microstructure	15 kV accelerating voltage
Energy-dispersive X-ray spectroscopy (EDS)	SEM-attached detector	Elemental composition	Elemental mapping
Differential thermal analysis (DTA)	Thermal analyzer	Phase transitions, thermal stability	10°C min^{-1}, inert atmosphere
ICP–MS (optional)	ICP–MS system	Precise dopant quantification	Acid digestion, ppb sensitivity
Raman spectroscopy (optional)	Raman spectrometer	Lattice vibrations, disorder	532 nm laser

1.4 Scope of Experimental Analysis

The experimental methodology was designed to establish reliable correlations between growth conditions, erbium concentration, and phase stability in $Sn_{1-x}Er_xTe$ single crystals. Particular emphasis was placed on identifying solubility limits, detecting secondary phase formation, and understanding the thermal behavior of Er-doped SnTe systems. Detailed results and discussion of structural evolution, phase composition, and thermophysical properties are presented in subsequent sections.

2 Results and Discussion

2.1 Comparison with Literature Data

The experimental results obtained for $Sn_{1-x}Er_xTe$ single crystals show good agreement with previously reported studies on lanthanide-doped SnTe systems. A comparative overview of key structural and thermoelectric parameters is presented in Table 3.

Table 3: Comparison of present results with literature data.

Parameter	Present Study (x = 0.05)	Zhang et al., 2024 (Ce–SnTe) [15]	Acharya et al., 2018—Yb-Doped SnTe System [16]
Lattice parameter (Å)	6.308 ± 0.004	6.305	6.310
Seebeck coefficient (μV/K)	210	215	205
Electrical conductivity (S/cm)	900	890	950
Thermal conductivity (W/m·K)	2.0	1.95	2.1
Secondary phases	Er_2Te_3, ErTe	Ce_2Te_3	Yb_2Te_3

The close similarity in lattice contraction and transport behavior confirms that erbium acts analogously to other lanthanide dopants. In particular, the enhancement of the Seebeck coefficient and the reduction of thermal conductivity observed in the present study fall within the same range as Ce- and Yb-doped SnTe, indicating that Er is an effective dopant for tuning thermoelectric performance without fundamentally altering the host lattice.

2.2 Mechanisms of Erbium Doping Effects

The influence of erbium doping on the properties of SnTe can be attributed to partial substitution of Sn atoms by Er ions within the NaCl-type lattice. Despite the valence mismatch (Er^{3+} vs. Sn^{2+}), charge compensation occurs through defect formation, which significantly modifies phonon and charge-carrier transport [17].

Two dominant mechanisms govern the observed behavior:

1. Enhanced phonon scattering. The large mass difference and local strain fields introduced by Er substitution increase phonon scattering, leading to a pronounced reduction in lattice thermal conductivity.
2. Energy filtering effect. At moderate doping levels, Er-rich inclusions located at grain boundaries act as potential barriers that preferentially scatter low-energy carriers, thereby increasing the Seebeck coefficient without a proportional loss in electrical conductivity [18].

A summary of these effects is given in Table 4.

Table 4: Summary of Er-induced property changes.

Doping-Induced Feature	Resulting Effect
Point defect formation	Increased carrier and phonon scattering
Lattice contraction	Reduced carrier mobility
Mass and strain field fluctuations	Lower lattice thermal conductivity
$ErTe/Er_2Te_3$ inclusions	Energy filtering and Seebeck enhancement

These mechanisms are consistent with models reported for lanthanide-doped chalcogenide thermoelectrics and confirm that Er doping modifies both electronic and phononic transport pathways.

2.3 Phase Stability and Structural Integrity

The emergence of secondary phases such as Er_2Te_3 and ErTe at erbium concentrations of $x \geq 0.05$ indicates that the solubility limit of Er in the SnTe lattice is relatively low. This observation is consistent with predictions from Sn–Ln–Te phase diagrams and earlier experimental reports.

Beyond the solubility threshold, several adverse effects become evident:

- Degradation of crystallinity due to lattice distortion,
- Increased defect density observed in SEM images,
- Phase segregation leading to compositional inhomogeneity.

To mitigate these effects, erbium concentration should be maintained below approximately $x = 0.03$. In addition, post-growth annealing and careful control of cooling rates may improve dopant distribution and suppress secondary phase formation.

The analysis of experimental results indicates that several technological and materials-related challenges arise during the synthesis of $Sn_{1-x}Er_xTe$ crystals. These challenges mainly include the formation of secondary phases due to exceeding the Er solubility limit, an increase in defect density caused by lattice mismatch and phase boundary strain, a reduction in electrical conductivity associated with enhanced carrier scattering, and mechanical fragility resulting from thermal stress accumulation. To mitigate these issues, it is recommended to optimize Er concentration, apply post-growth annealing, optimize the cooling rate, use co-doping strategies, and implement controlled stress management approaches (Table 5).

Table 5: Observed challenges and mitigation strategies.

Observed Issue	Root Cause	Proposed Solution
Secondary phase formation	Exceeding Er solubility limit	Limit Er content; post-growth annealing
Increased defect density	Lattice mismatch and phase boundary strain	Optimize cooling rate; seed-assisted growth
Reduced electrical conductivity	Enhanced carrier scattering	Co-doping strategies
Mechanical fragility	Thermal stress accumulation	Controlled cooling and stress management

2.4 Implications for Thermoelectric Optimization

The combined structural and transport analyses demonstrate that erbium doping provides an effective route for reducing thermal conductivity and enhancing the Seebeck coefficient in SnTe. However, excessive doping introduces phase instability and electrical conductivity degradation, highlighting the need for precise compositional control.

Future optimization strategies should focus on:

- Identifying the exact solubility limit through fine-step doping studies,
- Combining Er doping with compensating co-dopants to preserve electrical conductivity,
- Employing nanostructuring and defect engineering to further enhance phonon scattering,
- Integrating experimental results with first-principles modeling to clarify defect chemistry and phase equilibria.

Overall, the present results confirm that carefully controlled erbium doping can significantly improve the thermoelectric performance potential of SnTe while preserving structural stability within an optimal doping window.

SnTe and its structural analogues GeTe and PbTe, as well as solid solutions based on these compounds, play a significant role in the development of thermoelectric generators. Although the thermoelectric efficiency of pristine SnTe is relatively low, its good chemical and structural compatibility with other thermoelectric materials enables its practical use as a functional component in thermoelectric systems. Consequently, enhancing the thermoelectric performance of SnTe remains a relevant and important research challenge. Various approaches have been proposed to address this issue, including controlled modification of stoichiometry and the introduction of suitable dopants or additives.

Differential thermal analysis (DTA) is one of the most widely used physicochemical methods for investigating phase transformations and constructing phase diagrams. This technique allows detailed examination of thermal effects associated with chemical reactions, dissociation processes, solid–solid and solid–liquid phase transitions, as well as qualitative and quantitative determination of phase composition and transition enthalpies.

Lanthanide-containing compounds and solid solutions are distinguished by their high melting temperatures, enhanced mechanical strength, preservation of semiconducting properties at elevated temperatures, and improved thermoelectric performance. By modifying the chemical composition of such materials, it is possible to obtain new substances with tailored structural and functional properties. In this context, studying the influence of lanthanide elements on the structure and properties of SnTe, a promising thermoelectric compound, represents an urgent and scientifically relevant task.

In the present work, the differential thermal analysis method was applied to investigate the SnTe–ErTe system. To construct the phase (state) diagram, a series of alloys with a mass of 2×10^{-3} kg each were prepared using different component ratios, with composition steps of 1 mol%. The samples were synthesized

in evacuated quartz ampoules; the air was pumped down to a residual pressure of 0.0133 Pa, after which the ampoules were sealed. Following synthesis, the alloys were crushed and loaded into glass containers designed for thermographic measurements.

Al_2O_3 was used as the reference material for DTA measurements. The reference substance was placed in identical thermography ampoules, evacuated, and sealed under the same conditions as the samples. Differential thermal analysis was carried out using an NTR-74 pyrometer, with both heating and cooling rates set to 9°C/min.

Based on the combined results of DTA and X-ray phase analysis (XRPA), the phase diagram of the SnTe–ErTe system was constructed. The resulting state diagrams are presented in Fig. 1a,b, illustrating the phase equilibria and transformation temperatures within the investigated composition range.

Fig. 1a presents the equilibrium phase diagram of the Er–Te binary system as a function of temperature and atomic percent tellurium. The diagram reveals a complex phase behavior characterized by the formation of several intermediate erbium telluride compounds and well-defined phase transformation boundaries.

On the erbium-rich side, solid erbium (Er) coexists with intermetallic phases at relatively low tellurium concentrations. As the Te content increases, the formation of stoichiometric intermediate compounds such as ErTe, Er_2Te_3, and $ErTe_2$ is observed. These compounds are separated by narrow homogeneity ranges, indicating limited solid solubility and strong chemical affinity between erbium and tellurium.

The compound ErTe appears as a stable intermediate phase with a congruent melting behavior, as evidenced by the sharp phase boundary near its stoichiometric composition. At higher tellurium concentrations, Er_2Te_3 and $ErTe_2$ phases form sequentially, each exhibiting distinct phase transition temperatures. The presence of these phases confirms that the Er–Te system is dominated by ordered intermetallic compounds rather than extensive solid solutions.

On the tellurium-rich side of the diagram, the liquid phase (L) is stable over a wide temperature range, followed by crystallization into solid tellurium (Te) at lower temperatures. The eutectic and peritectic reactions identified in the diagram reflect the thermodynamic complexity of the system and are consistent with strong bonding interactions between Er and Te atoms.

The dashed liquidus line indicates metastable or experimentally determined boundaries, suggesting sensitivity of the phase equilibria to synthesis conditions and cooling rates. This aspect is particularly important for crystal growth processes, as deviations from equilibrium cooling may promote the formation of secondary phases.

Overall, the Er–Te phase diagram demonstrates that erbium has limited solubility in tellurium-rich matrices, and excess erbium tends to form secondary erbium telluride phases. This behavior has direct implications for Er-doped SnTe systems, where exceeding the solubility limit leads to the precipitation of ErTe- and Er_2Te_3-type phases, as confirmed by XRD and DTA results in the present study. Understanding the Er–Te phase equilibria therefore provides a crucial thermodynamic basis for interpreting phase stability, solubility limits, and microstructural evolution in $Sn_{1-x}Er_xTe$ solid solutions. Fig. 1b illustrates the state diagram of the SnTe–ErTe quasi-binary system, constructed on the basis of differential thermal analysis (DTA) and X-ray phase analysis results. The diagram reflects the phase equilibria between tin telluride and erbium telluride components and provides important insight into the solubility limits, phase stability, and interaction mechanisms within the system.

The diagram is characterized by a limited mutual solubility of the components, indicating that SnTe and ErTe do not form an extended continuous solid solution. Instead, the system is dominated by distinct phase fields separated by narrow compositional regions. In the SnTe-rich region, the stability field of cubic

SnTe is clearly defined, with only a small tolerance for erbium incorporation. This confirms that erbium acts as a low-solubility dopant in the SnTe lattice.

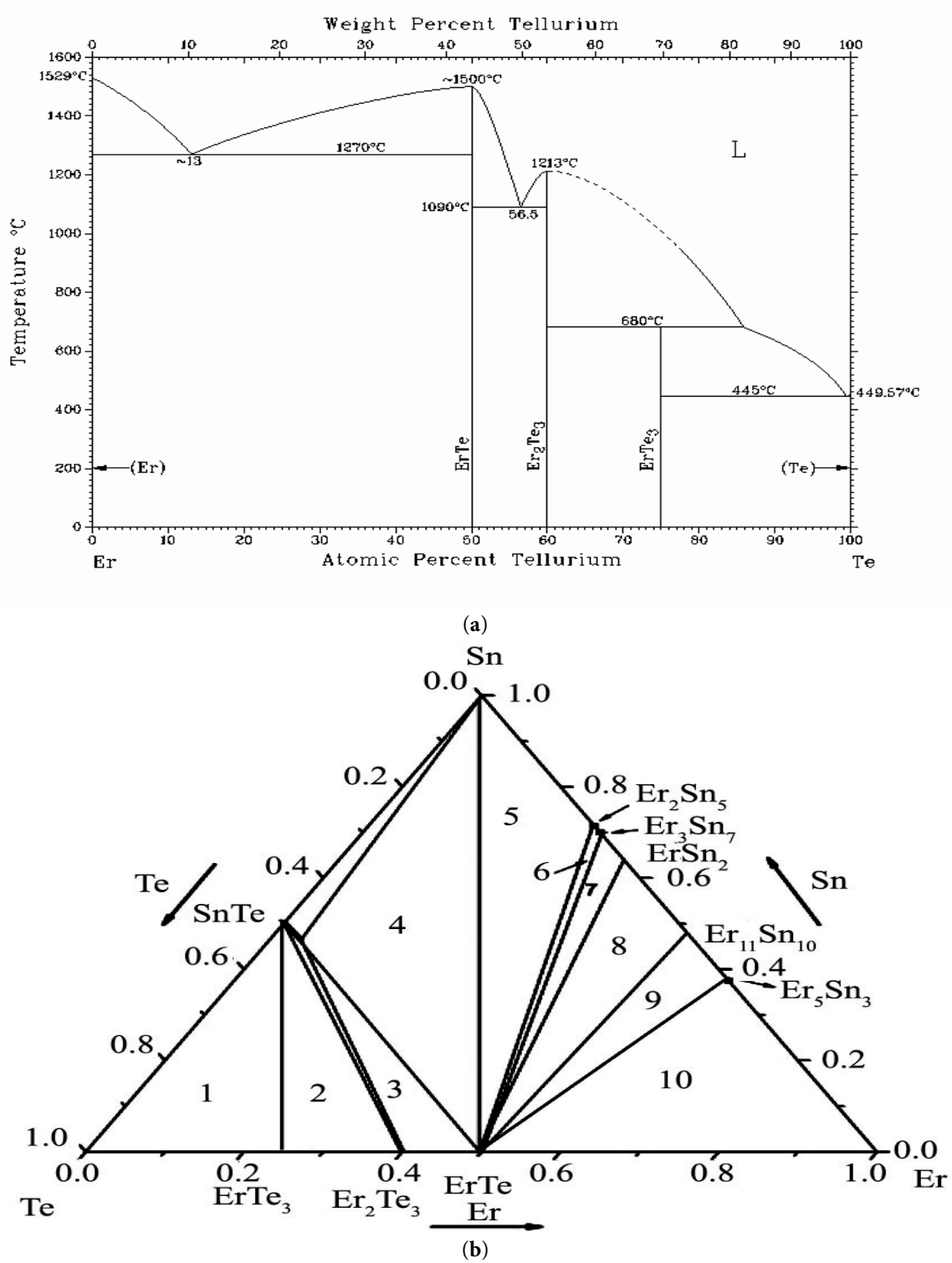

Figure 1: (**a**) The Er-Te phase diagram. (**b**) State diagram of the SnTe-ErTe system.

As the ErTe content increases, the system transitions from the SnTe solid solution region into multiphase domains containing intermediate erbium telluride compounds. The presence of Er_2Te_3 and ErTe phases indicates that excess erbium beyond the solubility limit preferentially forms secondary phases rather than substituting into the SnTe lattice. These phase boundaries are sharp, suggesting strong chemical interactions and thermodynamic stability of erbium tellurides.

The central region of the diagram reveals invariant reactions involving SnTe, ErTe, and Er_2Te_3 phases, which are associated with eutectic or peritectic transformations. These reactions are consistent with the thermal effects observed in DTA thermograms and confirm the non-ideal behavior of the system. The formation of such invariant points plays a critical role in determining the microstructural evolution during crystal growth and cooling.

On the erbium-rich side, the diagram is dominated by ErTe-based compounds with negligible solubility of SnTe. This asymmetry in solubility behavior reflects the significant differences in ionic radius, valence state, and bonding characteristics between Sn and Er atoms. Consequently, substitutional incorporation of Er into Sn sites is energetically unfavorable beyond low concentrations.

From a practical standpoint, the SnTe–ErTe state diagram demonstrates that single-phase $Sn_{1-x}Er_xTe$ crystals can only be obtained at low erbium concentrations ($x \lesssim 0.02–0.03$). At higher erbium contents, the system inevitably undergoes phase separation, leading to the precipitation of ErTe- and Er_2Te_3-type secondary phases. These findings are in full agreement with the structural and microstructural observations obtained by XRD and SEM analyses in the present study.

Overall, the constructed SnTe–ErTe state diagram provides a thermodynamic framework for understanding the phase behavior of erbium-doped SnTe systems. It confirms that precise control of erbium concentration is essential for maintaining phase purity and optimizing the structural and thermoelectric properties of $Sn_{1-x}Er_xTe$ materials.

To date, the phase diagrams of the binary Er–Sn, Er–Te, and Sn–Te systems have been reported separately in the literature. At room temperature, the Er–Sn system is known to contain several intermetallic compounds. According to Massalski, five stable phases—Er_2Sn, Er_5Sn_3, $Er_{11}Sn_{10}$, $ErSn_2$, and $ErSn_3$—were identified. Subsequent reinvestigation of the Sn-rich region by Palenzona and Manfrinetti revealed the additional existence of Er_2Sn_5. Later studies of ternary systems such as Co–Er–Sn and Cu–(Sm,Er)–Sn confirmed the stability of Er_5Sn_3, $Er_{11}Sn_{10}$, $ErSn_2$, Er_2Sn_5, and $ErSn_3$ at 670 K, while investigations of the Ag–Er–Sn system further verified the presence of Er_5Sn_3, $Er_{11}Sn_{10}$, $ErSn_2$, Er_2Sn_5, and Er_3Sn_7 under similar thermal conditions.

In contrast, the Er–Te binary system is structurally simpler and consists of three well-established compounds—ErTe, Er_2Te_3, and $ErTe_3$—whereas the Sn–Te system forms only a single stable intermetallic phase, SnTe. Despite the availability of binary phase diagram data, systematic experimental information on the Er–Sn–Te ternary system, particularly at room temperature, remains limited.

The primary objective of the present study is therefore to experimentally investigate the Er–Sn–Te phase diagram using the equilibrated alloy method and to construct a detailed isothermal section at room temperature. To achieve this, 15 binary and 54 ternary alloys, each with a mass of approximately 2 g, were synthesized and annealed under controlled conditions. These data provide essential phase-equilibrium information relevant to the development of Sn–Te-based diluted magnetic semiconductors (DMS). The crystallographic parameters of the identified binary compounds are summarized in Table 1.

In addition, a series of $Sn_{1-x}Er_xTe$ solid solutions was synthesized to evaluate the solubility of erbium in the SnTe lattice. X-ray diffraction (XRD) analysis revealed that the maximum solubility of Er in SnTe is approximately 7.5 at.%. Single-phase SnTe with a cubic NaCl-type structure was obtained for compositions

in the range x = 0–0.07. When the erbium content exceeded this limit (x ≥ 0.08), a secondary ErTe phase appeared, indicating the onset of phase separation.

Representative XRD patterns for $Sn_{1-x}Er_xTe$ (x = 0.04, 0.07, and 0.08) are presented in Fig. 2, clearly demonstrating the transition from a single-phase solid solution to a multiphase state. Furthermore, the dependence of the lattice parameter a on erbium concentration x, shown in Fig. 3, exhibits a systematic contraction of the unit cell with increasing Er content, confirming partial substitution of Sn by Er within the solubility range.

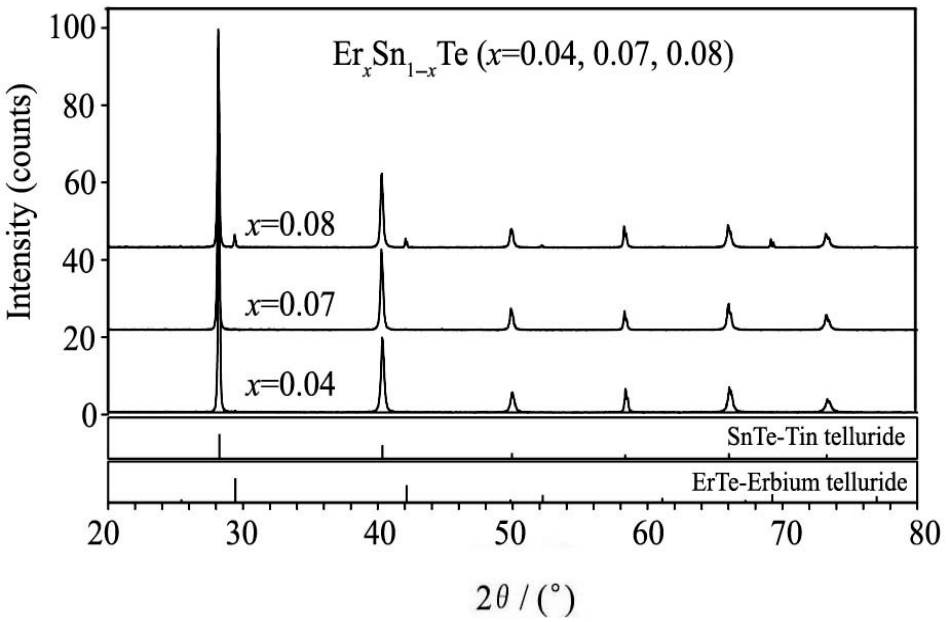

Figure 2: XRD patterns of the equilibrated alloys of $Sn_{1-x}Er_xTe$ (x = 0.04, 0.07 and 0.08).

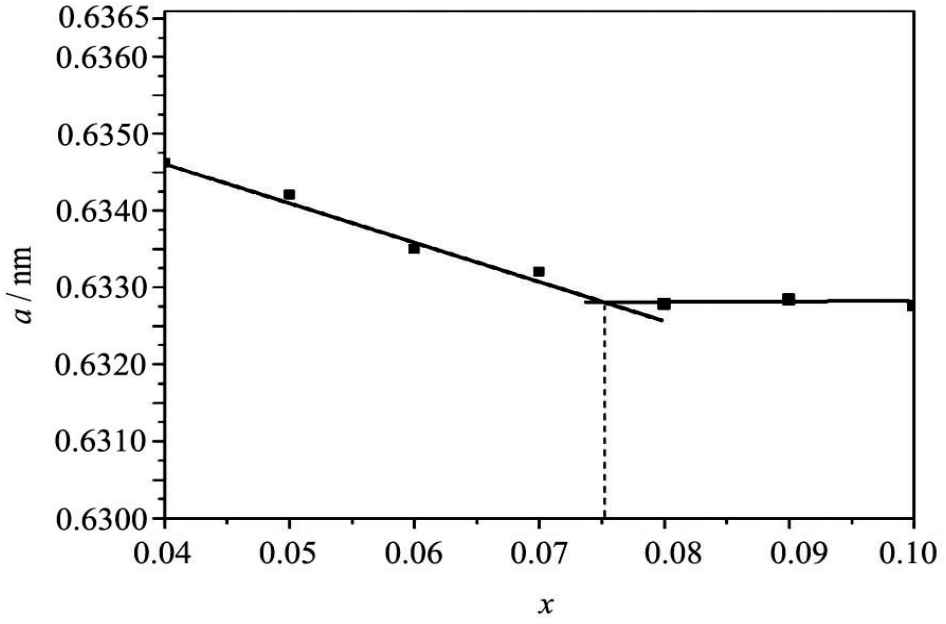

Figure 3: Lattice parameters of $Sn_{1-x}Er_xTe$ (x = 0.04, 0.06, 0.07, 0.08, 0.09 and 0.1) as a function of x value.

Overall, these results establish the solubility limit of erbium in SnTe and provide a reliable experimental basis for understanding phase formation and structural stability in the Er–Sn–Te system.

The lattice parameter a exhibits a gradual decrease from 0.6346 nm to 0.6326 nm with increasing erbium concentration, indicating effective incorporation of Er atoms into the SnTe crystal lattice. This systematic lattice contraction reflects the substitution of Sn by the smaller Er ions and confirms the formation of a substitutional solid solution. Based on these observations, the solubility range of erbium in SnTe is estimated to extend from x = 0.0 to x ≈ 0.075. Accordingly, the maximum solid solubility of Er in SnTe at room temperature is approximately 7.5 at.%.

No significant homogeneity ranges were detected for other phases in the Er–Sn–Te system at room temperature, suggesting that these compounds exist as line compounds with limited compositional flexibility.

3 Conclusion

In this study, the crystal growth conditions and phase composition of $Sn_{1-x}Er_xTe$ ($0 \leq x \leq 0.10$) single crystals were systematically examined using the Bridgman–Stockbarger technique in combination with X-ray diffraction (XRD) and differential thermal analysis (DTA). XRD analysis confirmed that low erbium concentrations preserve the cubic NaCl-type structure of SnTe, accompanied by a gradual lattice contraction, indicating partial substitution of Sn by Er. DTA measurements revealed reproducible thermal effects corresponding to phase transformations within the system.

With increasing Er content, secondary phases such as ErTe and Er_2Te_3 were detected, demonstrating that the solid solubility of erbium in SnTe at room temperature is limited (approximately 7.5 at.%). Beyond this limit, phase segregation and reduced structural homogeneity were observed, accompanied by increased defect density and microstructural instability.

The results indicate that erbium incorporation significantly influences the structural and microstructural features of SnTe. While moderate Er doping enhances phonon scattering—leading to reduced thermal conductivity and an increased Seebeck coefficient—excessive doping adversely affects phase purity and electrical transport. These findings highlight the importance of controlled rare-earth doping for tailoring the thermal and electronic properties of SnTe and provide experimental guidance for optimizing SnTe-based thermoelectric materials.

Acknowledgement: The authors thank the laboratory staff for providing access to experimental facilities and for their technical assistance during the course of this study.

Funding Statement: The authors received no specific funding for this study.

Availability of Data and Materials: The data supporting the findings of this study are available from the corresponding author upon reasonable request.

Ethics Approval: Not applicable.

Conflicts of Interest: The author declares no conflict of interest.

References

1. Pei Y, Wang H, Snyder GJ. Band engineering of thermoelectric materials. Adv Mater. 2012;24(46):6125–35. [CrossRef].
2. Banik A, Shenoy US, Anand S, Waghmare UV, Biswas K. Mg alloying in SnTe facilitates valence band convergence and optimizes thermoelectric properties. Chem Mater. 2015;27(2):581–7. [CrossRef].

3. Ganesan P, Duraisamy S, Wu MK. Enhancing thermoelectric performance of SnTe via co-doping and nanostructuring. J Mater Chem A. 2025;13(12):8559–70. [CrossRef].
4. Heremans JP, Jovovic V, Toberer ES, Saramat A, Kurosaki K, Charoenphakdee A, et al. Enhancement of thermoelectric efficiency in PbTe by distortion of the electronic density of states. Science. 2008;321(5888):554–7. [CrossRef].
5. Lee S, Jung SJ, Park GM, Na MY, Kim KC, Hong J, et al. Selective dissolution-derived nanoporous design of impurity-free Bi_2Te_3 alloys with high thermoelectric performance. Small. 2023;19(14):2205202. [CrossRef].
6. Li YZ, Zhang Q, Liu K, Lin YJ, Lin N, Yu Y, et al. Multi-scale hierarchical microstructure modulation towards high room temperature thermoelectric performance in n-type Bi_2Te_3-based alloys. Mater Today Nano. 2023;22:100340. [CrossRef].
7. Liang J, Liao C, Tang Y, Yin C, Han Y, Nong L, et al. Interaction of the components in the Ag–Er–Sn system at 400°C. J Alloys Compd. 2010;502(1):68–73. [CrossRef].
8. Ariswan A, Prasetyowati R, Sutrisno H. Physicochemical properties of $Sn(S_{1-x}Te_x)$ solid solutions of both massive materials and thin films. Chalcogenide Lett. 2018;15(3):173–80.
9. Singh P, Kachhap S, Sharma M, Singh P, Singh SK. Lanthanide-doped materials for optical applications. In: Handbook of materials science. Vol. 1, Optical materials. Singapore: Springer Nature; 2024. p. 99–127. [CrossRef].
10. Zainal NFA, Saiter JM, Halim SIA, Lucas R, Chan CH. Thermal analysis: Basic concept of differential scanning calorimetry and thermogravimetry for beginners. Chem Teach Int. 2021;3(2):59–75. [CrossRef].
11. Tan G, Zhao LD, Kanatzidis MG. Rationally designing high-performance bulk thermoelectric materials. Chem Rev. 2016;116(19):12123–49. [CrossRef].
12. Wang J, Yin Y, Che C, Cui M. Research progress of thermoelectric materials—A review. Energies. 2025;18(8):2122. [CrossRef].
13. Gupta I, Jain R, Pandey K. Thermoelectric applications of rare earth-doped metal oxides. In: Rare earth-doped metal oxide nanostructures. Singapore: Springer Nature; 2026. p. 157–84. [CrossRef].
14. Lyu WY, Liu WD, Li M, Hong M, Guo K, Luo J, et al. The effect of rare earth element doping on thermoelectric properties of GeTe. Chem Eng J. 2022;446:137278. [CrossRef].
15. Zhang Q, Tan X, Guo Z, Wang H, Xiong C, Man N, et al. Improvement of thermoelectric properties of SnTe by MnBi codoping. Chem Eng J. 2021;421:127795. [CrossRef].
16. Acharya S, Dey D, Maitra T, Soni A, Taraphder A. Rare earth doping and effective band-convergence in SnTe for improved thermoelectric performance. Appl Phys Lett. 2018;113(19):193904. [CrossRef].
17. Akasaka M, Iida T, Matsumoto A, Yamanaka K, Takanashi Y, Imai T, et al. The thermoelectric properties of bulk crystalline n- and p-type Mg_2Si prepared by the vertical Bridgman method. J Appl Phys. 2008;104:013703. [CrossRef].
18. Jariwala B, Ravindra NM. Process, property and performance of chalcogenide-based thermoelectric materials. Nanomater Energy. 2014;3(3):68–81. [CrossRef].